Research Square

Preprints are preliminary reports that have not undergone peer review.
They should not be considered conclusive, used to inform clinical practice,
or referenced by the media as validated information.

Targeting Arginine Metabolism via ARG2 Inhibition Improves Hypoxic CAR-T Cell Anti-Tumor Efficacy

Zhiying Chen

zhiyingxls@163.com

Nanjing Normal University College of Life Sciences: Nanjing Normal University School of Life Sciences

Zhengling Wang

Nanjing Normal University College of Life Sciences: Nanjing Normal University School of Life Sciences

Yuqi Zhao

Nanjing Normal University College of Life Sciences: Nanjing Normal University School of Life Sciences

Xiaoyu Li

Nanjing Normal University College of Life Sciences: Nanjing Normal University School of Life Sciences

Shenrui Zhou

Nanjing Normal University College of Life Sciences: Nanjing Normal University School of Life Sciences

Feiyan Pan

Nanjing Normal University College of Life Sciences: Nanjing Normal University School of Life Sciences

Zhigang Hu

Nanjing Normal University College of Life Sciences: Nanjing Normal University School of Life Sciences

Lingfeng He

Nanjing Normal University College of Life Sciences: Nanjing Normal University School of Life Sciences

Muya Zhou

Nanjing Normal University College of Life Sciences: Nanjing Normal University School of Life Sciences

https://orcid.org/0000-0002-2219-071X

Xiaodong Jiang

Lianyungang No 1 People's Hospital

Zhigang Guo

Nanjing Normal University College of Life Sciences: Nanjing Normal University School of Life Sciences

Research Article

Keywords: CAR-T cell therapy, Hypoxia, Arginase 2, Metabolic reprogramming, Memory phenotype

Posted Date: November 19th, 2026

DOI: https://doi.org/10.21203/rs.3.rs-11504552/v1

License: This work is licensed under a Creative Commons Attribution 4.0 International License.
Read Full License

Targeting Arginine Metabolism via ARG2 Inhibition Improves Hypoxic CAR-T Cell Anti-Tumor Efficacy

Zhiying Chen[1,†], Zhengling Wang[1,†], Yuqi zhao[1], Xiaoyu Li[1], Shenrui Zhou[1], Feiyan Pan[1], Zhigang Hu[1], Lingfeng He[1], Muya Zhou[1]*, Xiaodong jiang[2]*, Zhigang Guo[1]*

Zhiying Chen zhiyingxls@163.com Zhengling Wang wangzhengling2002@163.com Yuqi Zhao chelsea770220@163.com_Xiaoyu Li 13886996208@163.com Shenrui Zhou zsr919664117@163.com Feiyan Pan Panpanfeiyan@njnu.edu.cn Zhigang Hu huzg_2000@126.com , Lingfeng He lfhe22@139.com

*Correspondence to: Muya Zhou muyazhou@njnu.edu.cn Xiaodong jiangjxdysy1970@163.com and Zhigang Guo guo@njnu.edu.cn

† These authors contributed equally to this work.

Author Affiliations:

[1]Jiangsu Key Laboratory for Molecular and Medical Biotechnology, College of Life Sciences, Nanjing Normal University, 1 WenYuan Road, Nanjing, China, 210023.

[2]Lianyungang First People's Hospital (Affiliated Lianyungang Hospital of Xuzhou Medical University, Lianyungang Clinical College of Nanjing Medical University), Lianyungang, China, 222002.

Keywords: CAR-T cell therapy, Hypoxia, Arginase 2, Metabolic reprogramming, Memory phenotype

Declarations

Ethics approval and consent to participate

Animal experiments were conducted at the animal laboratory of Nanjing Normal University in strict compliance with the ARRIVE 2.0 guidelines and in accordance with protocols approved by the Animal Welfare Committee of the university (Approval number: 2020-0047).

Consent for publication

Not applicable. This study does not contain any individual person's data in any form (including individual details, images, or videos).

Availability of data and material

All data generated or analyzed during the study are included in the paper or its online supplemental information, or available upon request. The RNA-seq raw data presented in this study have been deposited in the NCBI repository under the accession number PRJNA1435635.

Competing interests

All the authors declare no conflict of interest.

Funding

This work was supported by the National Natural Science Foundation of China (82373183), the Priority Academic Program Development of Jiangsu Higher Education Institutions and Jiangsu Funding Program for Excellent Postdoctoral Talent (2024ZB561).

Authors' contributions

Methodology, software and investigation: Zhigang Hu, Muya Zhou; validation and formal analysis: Zhiying Chen, Zhengling Wang, Yuqi Zhao, Shenrui Zhou; resources: Feiyan Pan, Zhigang Hu, Muya Zhou, Zhigang Guo; data curation: Xiaoyu Li, Shenrui Zhou; writing—original draft preparation: Zhiying Chen, Zhengling Wang; writing—review and editing: Muya Zhou, Zhigang Guo, Zhiying Chen, Zhengling Wang; visualization: Yuqi Zhao, Xiaoyu Li; supervision, project administration and funding acquisition: Muya Zhou, Zhigang Guo. All authors have read and agreed to the published version of the manuscript.

Acknowledgements

We thank the members of our laboratory for their valuable discussions and technical support throughout this study. We also appreciate the assistance provided by the core facilities from Nanjing Normal University and Nanjing University for flow cytometry, animal studies, and metabolomics analysis.

Abstract

Background: Tumor hypoxia is a major metabolic barrier that limits CAR-T cell persistence and antitumor efficacy in solid tumors. Here, we identify arginase 2 (ARG2) as a critical cell-intrinsic mediator of hypoxia-induced CAR-T cell dysfunction.

Methods: Using MSLN and CD70 specific CAR-T cells, we evaluated three complementary strategies to target ARG2: pharmacological inhibition with BEC, extracellular L-arginine supplementation, and CRISPR-Cas9-mediated ARG2 knockout. CAR-T cell function, exhaustion, and memory differentiation were assessed under hypoxic conditions (1% O_2) by serial killing assays, cytokine detection, and flow cytometry. In vivo efficacy was evaluated in a xenograft tumor model, and transcriptomic profiling was performed to delineate underlying molecular mechanisms.

Results: Hypoxia markedly upregulated ARG2 expression in CAR-T cells independent of antigen specificity. Pharmacological ARG2 inhibition with BEC (10 μM) restored sustained cytotoxicity and pro-inflammatory cytokine secretion (IFN-γ and TNF-α), reduced exhaustion markers (PD-1 and LAG-3), and promoted a durable memory phenotype by enriching stem cell memory (TSCM) and central memory (TCM) subsets while decreasing terminal effector (TTE) cells. L-arginine supplementation (2 mM) similarly enhanced cytotoxic function and alleviated exhaustion but failed to remodel memory differentiation, indicating mechanistic distinctions between substrate replenishment and enzymatic blockade. Genetic ARG2 knockout recapitulated these protective effects, preserving cytolytic activity and

increasing $CD62L^+$ memory-like populations under hypoxia. In vivo, both BEC- and L-Arg-pretreated CAR-T cells improved tumor control, enhanced circulating persistence, reduced exhausted T cell frequencies, and increased intratumoral $CD45^+$ infiltration without overt toxicity, with BEC specifically elevating TCM proportions. Transcriptomic analysis revealed that ARG2 ablation triggered broad transcriptional reprogramming, with enrichment of PI3K-AKT signaling, stem cell pluripotency pathways, and glycine/serine/threonine metabolism. IGF2, a well-documented upstream activator of the PI3K-AKT axis, was significantly upregulated in ARG2-deficient cells at both the transcriptomic and qPCR validation levels, suggesting it may serve as a downstream mediator of ARG2 deficiency that drives PI3K-AKT pathway activation.

Conclusions: These findings establish ARG2 as a pivotal regulator of hypoxia-driven CAR-T cell dysfunction and support ARG2-targeted interventions—particularly pharmacological inhibition—as a promising strategy to enhance metabolic fitness, memory phenotype, and therapeutic durability against solid tumors.

Background

Although CAR-T cell therapy has demonstrated remarkable efficacy against hematological malignancies, its translation to solid tumors remains substantially limited. Among the various obstacles, tumor hypoxia represents a prevalent and critical immunosuppressive factor in the tumor microenvironment, significantly compromising the survival, tumor infiltration, cytotoxic function, and metabolic adaptability of CAR-T cells in vivo [1–4]. Hypoxia not only reshapes tumor cell

behavior to facilitate immune evasion but also induces T-cell exhaustion and metabolic disturbance, thereby further attenuating the antitumor activity of CAR-T cells [5–7]. Therefore, overcoming hypoxia-mediated CAR-T cell dysfunction represents a critical strategy to improve immunotherapeutic outcomes against solid tumors.

To mitigate the detrimental effects of hypoxia on CAR-T cells, researchers have developed various genetic and pharmacological strategies, including hypoxia-responsive CAR constructs, ectopic expression of cytokines or chimeric switch receptors, and modulation of hypoxia-inducible factor (HIF) signaling [8–10]. These approaches have shown promise in preserving T-cell survival and transcriptional adaptation under hypoxic stress. However, hypoxia concurrently imposes profound metabolic constraints on T cells including impaired oxidative phosphorylation and altered amino acid metabolism [11], which are not directly addressed by strategies focused primarily on CAR expression or signaling rewiring. Given that T-cell effector function is tightly coupled to metabolic fitness [12,13], interventions that correct hypoxia-induced metabolic dysregulation may offer a complementary avenue to enhance CAR-T cell performance in solid tumors.

Arginine metabolism represents a particularly attractive target in this context. As a conditionally essential amino acid, arginine is required for T-cell receptor signaling, cellular biomass accumulation, and cytokine production, yet its intracellular availability is rapidly compromised under hypoxic stress through enhanced catabolism. Arginase 2 (ARG2) is a mitochondrial enzyme that is highly induced

under hypoxic stress and catalyzes the catabolism of arginine into ornithine and urea, thereby depleting intracellular arginine pools [14,15]. Accumulating evidence indicates that ARG2-mediated arginine depletion suppresses antitumor immune responses and promotes an immunosuppressive phenotype [16]. However, whether hypoxia-induced ARG2 upregulation directly drives CAR-T cell dysfunction in solid tumors, and whether metabolic intervention targeting arginine availability can rescue CAR-T cell efficacy under hypoxic conditions, remain to be elucidated.

In this study, we first observed that ARG2 expression was markedly upregulated in CAR-T cells following prolonged hypoxic culture. Based on this finding, we hypothesized that hypoxia-driven ARG2 upregulation accelerates arginine catabolism, thereby impairing the effector function of CAR-T cells. To test this hypothesis, we employed three complementary strategies: pharmacological inhibition of ARG2 activity with BEC, extracellular L-arginine supplementation to restore arginine availability, and CRISPR-Cas9-mediated ARG2 knockout to comprehensively evaluate the role of ARG2 in hypoxia-induced CAR-T cell dysfunction. In parallel, we performed transcriptomic profiling to further explore the underlying molecular mechanisms. This study aims to determine whether targeting ARG2 can alleviate hypoxia-induced CAR-T cell dysfunction and enhance their antitumor efficacy against solid tumors, thereby providing a rationale for optimizing CAR-T immunotherapy.

Methods

Cell lines and culture

Human breast cancer cell line HCC1806 and human ovarian cancer cell line

OVCAR3 were obtained from the American Type Culture Collection (ATCC). Stable cell lines expressing firefly luciferase (ffluc) were generated via lentiviral transduction of HCC1806, OVCAR3 and HEK293T cells, and were termed HCC1806-luc, OVCAR3-luc and HEK293T-luc, respectively. HEK293T-luc cells were maintained in Dulbecco's Modified Eagle Medium (DMEM, Gibco) containing 10% fetal bovine serum (FBS). OVCAR3-luc and HCC1806-luc cells were cultured in Roswell Park Memorial Institute 1640 medium (RPMI-1640, Gibco) supplemented with 10% FBS. During the expansion and drug treatment phases, cells were maintained under normoxic conditions (21% O_2). Following completion of these treatments, cells were transferred to hypoxic conditions (1% O_2) for subsequent functional assessments. All cells were incubated at 37 ℃ in a humidified atmosphere containing 5% CO_2.

The generation of CAR-T cells

CAR-T cell generation followed established protocols [16]. Chimeric antigen receptors specific for MSLN or CD70 were engineered by fusing proprietary fully human single-chain variable fragments (scFvs) to a CD8α signal peptide, followed by hinge and transmembrane regions, and a CD28/CD3ζ intracellular signaling domain; the complete construct was subcloned into the pCDH lentiviral vector. Primary human T cells were enriched from peripheral blood mononuclear cells (PBMCs; HYCELLS, hPB050C) via negative immunomagnetic selection using the EasySep™ Human T-Cell Isolation Kit (Stemcell, 17951). Isolated T cells were stimulated with

Dynabeads™ Human T-Expander CD3/CD28 beads (Thermo Fisher Scientific, 11141D) at a 1:1 bead-to-cell ratio, and 24 hours post-activation, transduced with VSV-G-pseudotyped lentiviral particles (produced in HEK293T cells) encoding the respective CAR to establish MSLN- or CD70-targeting CAR-T cells. Following transduction, cells were maintained in X-VIVO medium (LONZA) containing 100 IU/mL recombinant human IL-2; culture medium was replenished every 2–3 days to sustain cell concentrations between 0.5 and 1×10^6 cells/mL.

Flow cytometry

The following fluorochrome-conjugated antibodies were purchased from Biolegend and employed in this study: APC-anti-PD-1, FITC-anti-LAG-3, PE-anti-CD62L, APC-anti-CD45RO, PE-anti-CD69, and APC-anti-CD25. For human anti-MSLN CAR detection, PE-conjugated recombinant human MSLN protein (KACTUS) was utilized as the detection reagent. Additionally, FITC-labeled human CD27 Ligand/CD70 Trimer protein (Kairui Biology, CDL-HM427F-100μg) was used to detect CAR expression targeting CD70.

For flow cytometric analysis of cell-surface markers, cells were stained with the indicated antibodies at room temperature for 20 min, followed by washing with phosphate-buffered saline (PBS). Acquisition was performed on a CytoFLEX S flow cytometer (Beckman Coulter), and subsequent data analysis was conducted using CytExpert software.

Cytotoxicity assays

To evaluate the sustained killing capacity of CAR-T cells, a sequential tumor cell rechallenge assay was performed. Preconditioned CAR-T cells were cocultured with tumor cells at the indicated effector-to-target (E:T) ratios for 24 h; the T cells were then harvested and replated onto fresh tumor cell cultures for an additional 24-h coculture. This procedure was carried out for three consecutive rounds, with cytotoxic activity assessed following each round.

Tumor cell lysis was quantified using the One-Lite Luciferase Assay System (Vazyme, DD1203-02) per the manufacturer's protocol. The cell killing rate was calculated as follows: (control value − experimental value) / control value × 100%.

Cytokine release detection

Cytokine levels in CAR-T cell culture supernatants and mouse blood plasma were measured using a cytometric bead array (CBA) kit (BD Pharmingen, 558264) according to the manufacturer’s protocol. Briefly, capture beads specific for TNF-α (BD Pharmingen, 558273) and IFN-γ (BD Pharmingen, 560111) were pooled and incubated with the samples for 1 hour. Subsequently, detection reagent was added and the mixture was incubated for an additional 2 hours. After careful washing, the beads were resuspended in phosphate-buffered saline (PBS). Samples were acquired on a flow cytometer, and the data were analyzed using FCAP Array software.

Animal experiments

All animal procedures were performed at the Animal Experiment Center of Nanjing Normal University, following protocols approved by the Institutional Animal Welfare Committee (Approval No. 2020-0047). Eight-week-old female NXG mice, obtained from Hangzhou Qizhen Laboratory Animal Technology Co., Ltd., were used in this study. Each mouse received a subcutaneous injection of 2×10^6 HCC1806-luc cells. Treatment began on day 12 after tumor inoculation. For CAR-T cell therapy, 1×10^6 CAR-T cells suspended in 100 μL of vehicle were administered via tail vein injection into each mouse. On day 10 following CAR-T infusion, peripheral blood was collected. Mice were then euthanized on day 24 for tissue harvest, and the collected samples were subjected to flow cytometry and immunohistochemistry(IHC). Throughout the experimental period, tumor volume and body weight of HCC1806-bearing mice were measured and recorded every other day. Tumor volume was calculated using the formula: volume = (length × width²) / 2.

Analysis of tissue samples

AiFang Biological performed IHC. For histopathological evaluation, mouse tissues were fixed in 4% paraformaldehyde, paraffin-embedded, sectioned (4 μm), and stained with hematoxylin and eosin (H&E). For immunostaining, sections were deparaffinized, rehydrated, processed for antigen retrieval, and blocked in 3% BSA. Slides were then incubated overnight at 4 ℃ with an anti-human CD45 primary antibody, followed by secondary antibody incubation, counterstaining with hematoxylin, and mounting. Whole-slide images were acquired with a digital slide

scanner and analyzed using ImageJ.

Real-time quantitative polymerase chain reaction (qPCR)

Total RNA was isolated from collected cells using the FastPure Cell/Tissue Total RNA Isolation Kit V2 (Vazyme, RC112). The HiScript III 1st Strand cDNA Synthesis Kit (+gDNA wiper) (Vazyme, R312) was employed for reverse transcription according to the manufacturer's instructions. qPCR was then conducted with the 2×Taq Pro Universal SYBR qPCR Master Mix (Vazyme, Q712). The primer sequences are listed in Table 1.

Table 1. Primers used for RT-qPCR analysis of gene expression in CAR-T cells.

Gene	Primer sequences (5'→3')
ARG2	F:ACCTGATAGTGAATCCACGCT
	R:CATGGGCATCAACCCAGAC
IGF2	F:CCCGTGGGCAAGTTCTTCC
	R:CGCTGGGTGGACTGCTTC

ARG2 knockout (KO)

ARG2 knockout (ARG2 KO) cells were generated using the CRISPR/Cas9 system. Briefly, 60 pmol of Cas9 protein was mixed with 100 pmol of sgRNA (sequences listed in Table 2, General Biosystems) to form the ribonucleoprotein (RNP) complex, which was incubated at room temperature for 10 min. A total of 2×10^6 CAR-T cells

were resuspended in electroporation buffer, mixed with the RNP complex, and electroporated using a Lonza nucleofector device. Immediately after electroporation, the cell suspension was diluted with pre-warmed complete medium and incubated statically at 37 °C for 15 min, followed by transfer to a 12-well plate for culture. After 48 h, the cells were transferred to a 6-well plate and maintained at a density of 1×10^6 cells/mL, with medium replacement every 48 h.

Table 2. sgRNA sequences used for CRISPR-Cas9-mediated ARG2 knockout in CAR-T cells.

Gene	Primer sequences (5'→3')
Arg2#1	TAGGAGCCCCGTTCTCACAA
Arg2#2	GCGTCTGGAGGAGACGCGAG

Western blot

Cells were lysed in RIPA buffer with protease inhibitors, centrifuged at 12,000 rpm for 10 min at 4°C, and supernatants were quantified by BCA assay. After denaturation at 100°C for 10 min, samples (10 μL) were resolved by SDS-PAGE (80 V for stacking gel, 120 V for separating gel) and transferred to ethanol-activated PVDF membranes at 260 mA. Membranes were blocked with 5% skim milk in TBST for 2 h at room temperature, then incubated overnight at 4°C with anti-ARG2 (Youpin, YP-Ab-03711, 1:1000 in 5% BSA), followed by HRP-conjugated secondary antibody (PTG, RGAM001, 1:2000) for 2 h at room temperature, with three 10-min TBST washes after each antibody step. Bands were visualized by ECL, after which membranes were stripped with neutral stripping buffer (Biosharp) for 10 min, re-probed with

anti-GAPDH (PTG, rabbit, 10494-1-AP), and re-imaged. Band intensities were quantified using ImageJ and normalized to GAPDH.

RNA-sequencing

Wild-type and ARG2 knockout CAR-T cells were cultured under hypoxic conditions for 6 days. From each cell type, 1×10^6 cells were collected, washed with PBS, and resuspended in TRIzol reagent. The samples were then submitted to LC-Bio Technologies for transcriptome sequencing (RNA-seq). The RNA-seq raw data presented in this study have been deposited in the NCBI repository under the accession number PRJNA1435635.

Statistical analysis

All data analyses and figure preparation were performed with GraphPad Prism 10.1.2. Statistical comparisons were conducted using two-tailed unpaired Student's t-tests, one-way ANOVA, or two-way ANOVA as appropriate to the experimental design. Statistical significance was set at $P < 0.05$. Data are expressed as mean ± SD unless otherwise stated.

Results

Hypoxia-induced ARG2 upregulation in CAR-T cells

Hypoxia constitutes a prominent metabolic barrier limiting the in vivo persistence and anti-tumor potency of CAR-T cells within solid tumor microenvironments. Our

previous RNA-seq performed on CAR-T cells revealed that hypoxia significantly upregulated ARG2 transcription under hypoxic culture (Figure 1A). To further verify this phenotype across distinct CAR formats, we generated an additional CD70-specific CAR-T cell line; both MSLN-CAR and CD70-CAR shared identical intracellular signaling backbone (Figure 1B). Flow cytometry confirmed robust CAR surface expression in both cell populations, with 71.53% $CAR^+$for MSLN CAR-T and 82.34% $CAR^+$for CD70 CAR-T, whereas negligible CAR signal was detected in unmodified mock T cells, confirming successful construction of the two CAR-T models (Figure 1C, D). After 12 days of routine in vitro expansion, both CAR-T subsets were split and cultured under normoxic (21% O_2) or hypoxic (1% O_2) conditions for another 6 days (Figure 1E). Consistent with the earlier transcriptomic data, qPCR results demonstrated that ARG2 mRNA levels were markedly and significantly elevated under hypoxia in both MSLN CAR-T and CD70 CAR-T groups relative to their normoxic counterparts (Figure 1F). Collectively, these results confirm that hypoxia robustly induces ARG2 upregulation in CAR-T cells independent of antigen specificity.

Pharmacological inhibition of ARG2 by BEC restores the anti-tumor function of CAR-T cells under hypoxic conditions

To determine whether targeting ARG2-mediated arginine metabolism reverses hypoxia-induced CAR-T cell dysfunction, we employed two strategies: pharmacological inhibition with BEC and extracellular L-arginine supplementation

(Figure 2A).

We first evaluated BEC toxicity on CAR-T cell proliferation. Exposure to 5, 10, or 20 μM BEC for 6 days did not perturb growth kinetics (Figure 2B). Flow cytometric analysis further confirmed that BEC treatment did not compromise CAR transduction efficiency: while 5 μM BEC produced a modest but statistically significant increase in CAR-positive rates, 10 μM and 20 μM remained comparable to the control group (Figure S1A). All three doses were thus advanced to functional assays.

Prior to hypoxic functional testing, we confirmed that MSLN CAR-T cells mediated strictly antigen-specific cytotoxicity, exhibiting potent lysis against MSLN-positive 1806 and OVCAR3 tumor cells but minimal background cytotoxicity against MSLN-negative 293T cells (Figure S1B-C). Under serial tumor challenge against these MSLN-positive targets, control CAR-T cells progressively lost cytotoxic activity under hypoxia, whereas BEC treatment improved sustained antitumor activity, with 10 μM showing the most prominent rescue effect (Figure 2C). BEC-treated cells also exhibited enhanced IFN-γ and TNF-α secretion upon tumor coculture (Figure 2D–E). Based on these proliferation, cytotoxicity, and cytokine data, 10 μM was selected for subsequent phenotypic analyses.

At this concentration, BEC significantly reduced exhaustion markers PD-1 and LAG-3 (Figure 2F) and downregulated activation markers CD25 and CD69 (Figure 2G). Memory subset analysis further demonstrated increased proportions of stem cell memory (T_{SCM}) and central memory (T_{CM}) cells, alongside decreased effector memory (T_{EM}) and terminal effector (T_{TE}) populations (Figure 2H).

Collectively, pharmacological inhibition of ARG2 by BEC restores cytotoxic function and cytokine secretion, alleviates T cell exhaustion, modulates activation marker expression, and promotes a more durable memory phenotype in hypoxic CAR-T cells.

L-Arginine Supplementation Enhances Antitumor Function and Modulates Phenotypic Profiles of CAR-T Cells In Vitro

In a complementary approach, we investigated whether extracellular L-arginine (L-Arg) supplementation, a substrate replenishing strategy that bypasses ARG2-mediated arginine depletion, could restore CAR-T cell function under hypoxic conditions.

To establish an appropriate dosing regimen, we first assessed the effect of L-Arg on CAR-T cell proliferation. Addition of 1, 2, and 5 mM L-Arg for 6 days left cell growth kinetics unaffected (Figure 3A). Flow cytometric analysis further confirmed that L-Arg supplementation did not compromise CAR transduction efficiency, as CAR-positive rates remained comparable across all supplemented groups and controls (Figure S1D). These concentrations were therefore used in subsequent functional assays. L-Arg was administered from day 6 to day 11 post-transfection, after which the medium was replaced to remove residual amino acid, and cells were transferred to hypoxic conditions (1% O_2) for further analysis.

When subjected to serial tumor challenge, control CAR-T cells showed progressive loss of cytotoxic activity under hypoxia across three rounds against both OVCAR3 and 1806 cells. L-Arg supplementation improved the sustained killing capacity of

CAR-T cells under hypoxic conditions, with 2 mM L-Arg exhibiting the most pronounced rescue effect among the three concentrations tested, although all supplemented groups outperformed the untreated control (Figure 3B).

Cytokine profiling further showed that L-Arg supplementation increased IFN-γ and TNF-α secretion by hypoxic CAR-T cells upon coculture with tumor cells. However, the magnitude of enhancement varied across cell lines and concentrations, with 2 mM L-Arg showing a relatively balanced response (Figure 3C-D). Accordingly, 2 mM L-Arg was selected for subsequent phenotypic analyses.

In contrast to the effects of BEC on memory differentiation, 2 mM L-Arg treatment reduced the surface expression of exhaustion markers PD-1 and LAG-3 (Figure 3E), and also significantly downregulated activation markers CD25 and CD69 (Figure 3F). However, L-Arg did not significantly alter memory subset distribution based on CD62L and CD45RO expression, including stem cell memory (T_{SCM}), central memory (T_{CM}), effector memory (T_{EM}), and terminal effector (T_{TE}) cells (Figure 3G-H).

Taken together, extracellular L-Arg supplementation partially restores the effector function of hypoxic CAR-T cells, as evidenced by improved serial killing activity, enhanced cytokine secretion, and reduced exhaustion marker expression. Nevertheless, unlike pharmacological ARG2 inhibition, L-Arg supplementation does not significantly affect memory differentiation, suggesting that the two strategies operate through distinct mechanisms. Exogenous L-arginine merely increases substrate availability to transiently fuel effector machinery, whereas BEC directly suppresses

cell-intrinsic ARG2 activity and thereby rewrites endogenous metabolic and transcriptional programs. Because hypoxia-driven ARG2 overexpression actively hydrolyzes intracellular arginine, extracellular supplementation alone cannot override this intrinsic metabolic shunt or elicit the sustained transcriptional reprogramming required for memory subset commitment. Thus, L-arginine rescues acute effector function by replenishing substrate, whereas ARG2 inhibition reprograms T cell fate by interrupting a cell-autonomous metabolic checkpoint.

Genetic ablation of ARG2 enhances effector function and preserves memory phenotype of CAR-T cells under hypoxic stress

Having established that both pharmacological inhibition of ARG2 and exogenous L-arginine supplementation rescue CAR-T cell function under hypoxia, we next employed CRISPR-Cas9-mediated gene editing to genetically validate ARG2 as a causal mediator of hypoxia-induced CAR-T cell dysfunction and to determine whether genetic ablation recapitulates the protective effects observed with pharmacological intervention. The experimental workflow is outlined in Figure 4A.

We first verified knockout efficiency at the transcript and protein levels. Quantitative PCR analysis demonstrated that ARG2 mRNA expression was substantially reduced in two independent ARG2 knockout CAR-T cell clones (ARG2 KO#1 and ARG2 KO#2) relative to wild-type (WT) controls under hypoxic conditions (Figure 4B). Western blotting confirmed diminished ARG2 protein abundance in both KO clones (Figure 4C). Densitometric quantification revealed that ARG2 KO#2 achieved

statistically significant protein knockdown, whereas ARG2 KO#1 exhibited a consistent downward trend that did not reach statistical significance, indicative of partial ARG2 depletion (Figure 4D).

We next assessed the phenotypic consequences of ARG2 deletion in CAR-T cells cultured under hypoxia. Flow cytometric analysis showed that ARG2 knockout significantly decreased the proportion of cells expressing the exhaustion markers PD-1 and LAG-3 (Figure 4E), indicating that loss of ARG2 attenuates hypoxia-driven T cell exhaustion. Regarding activation markers, ARG2 KO cells displayed a modest increase in surface CD25 expression, whereas CD69 levels remained comparable between WT and knockout groups (Figure 4F). Moreover, memory phenotype analysis revealed a significant expansion of CD62L positive cells in ARG2 deficient cultures (Figure 4G), consistent with a shift toward a long-lived memory-like state.

We further evaluated the functional impact of ARG2 deletion using serial tumor challenge assays under hypoxic conditions. WT CAR-T cells exhibited progressive loss of cytotoxic capacity across three rounds of stimulation with OVCAR3 and 1806 tumor cells. In contrast, both ARG2 KO clones maintained robust sustained cytolytic activity, achieving significantly higher tumor lysis rates than WT controls by the third round of challenge (Figure 4H). Consistent with these cytotoxicity findings, ARG2-deficient CAR-T cells secreted significantly elevated levels of the effector cytokines TNF-α and IFN-γ upon tumor cell co-culture under hypoxia (Figure 4I).

Collectively, genetic disruption of ARG2 recapitulates the phenotypic and functional benefits observed with pharmacological ARG2 inhibition. Notably, despite variable

protein knockdown efficiencies between sgRNAs, both conferred consistent protective effects, indicating that even partial reduction of ARG2 expression is sufficient to ameliorate hypoxia-induced CAR-T cell dysfunction. These genetic data establish ARG2 as a key mediator of hypoxia-induced CAR-T cell dysfunction and support the translational potential of pharmacological ARG2 targeting.

Pharmacological targeting of ARG2 improves CAR-T cell antitumor efficacy in vivo

Having established ARG2 as a causal mediator of hypoxia-induced CAR-T cell dysfunction through CRISPR-mediated knockout in vitro, we elected to prioritize pharmacological strategies for in vivo translation, as BEC and L-arginine represent clinically actionable ex vivo conditioning regimens with well-defined safety profiles and shorter translational paths. We therefore evaluated whether these pretreatments could enhance CAR-T cell mediated tumor control in an immunodeficient xenograft model. The in vivo experimental schedule is illustrated in Figure 5A. 1806 tumor bearing mice received intravenous adoptive transfer of control CAR-T cells, BEC pretreated CAR-T cells, or L-Arg pretreated CAR-T cells.

Tumor growth monitoring revealed that CAR-T cell therapy attenuated tumor progression relative to the PBS control group. Notably, both BEC and L-Arg pretreated CAR-T cells conferred superior tumor growth suppression compared with control CAR-T cells (Figure 5B–C). To assess CAR-T cell persistence, we quantified circulating CAR-T cells in peripheral blood at day 10 post-transfer. Both pretreatment

regimens resulted in higher CAR-T cell numbers in peripheral blood, suggesting enhanced in vivo retention at this time point (Figure 5D).

We next characterized the exhaustion status of circulating CAR-T cells. Both BEC and L-Arg pretreatment markedly reduced the frequencies of PD-1 and LAG-3 positive exhausted CAR-T cells (Figure 5E). Consistent with our in vitro findings, the BEC-pretreated group exhibited an elevated proportion of central memory T (T_{CM}) cells and a concomitant reduction in terminal effector T (T_{TE}) cells; by contrast, L-Arg pretreatment did not significantly alter memory subset distribution (Figure 5F–G).

Immunohistochemical analysis of tumor tissues revealed markedly increased intratumoral $CD45^+$ lymphocyte infiltration in both the BEC and L-Arg groups relative to the control CAR-T group. Quantitative assessment of CD45 staining further confirmed enhanced tumor-infiltrating human T-cell abundance following either pretreatment (Figure 5H–I).

No significant body weight loss was observed across experimental groups throughout the observation period (Figure 5J). Histopathological examination of major organs (heart, liver, spleen, lung, kidney, and brain) by hematoxylin and eosin (H&E) staining showed no overt tissue damage or inflammatory lesions in any group (Figure S1D), indicating that these pretreatment regimens did not induce discernible organ-related toxicity under the conditions tested.

Collectively, these in vivo data demonstrate that pharmacological targeting of ARG2 whether by BEC-mediated inhibition or L-arginine supplementation enhances CAR-T cell antitumor efficacy, promotes circulating CAR-T cell persistence, alleviates T-cell

exhaustion, and increases tumor-infiltrating lymphocyte accumulation in the xenograft model.

Transcriptomic profiling uncovers perturbed signaling and metabolic programs in ARG2 knockout CAR-T cells

To delineate the molecular mechanisms underlying the enhanced effector function of ARG2-deficient CAR-T cells under hypoxia, we performed RNA sequencing on wild-type and ARG2 knockout CAR-T cells cultured under hypoxic conditions.

Volcano plot analysis revealed widespread differential gene expression between the two groups, with 122 genes significantly upregulated and 56 genes significantly downregulated in ARG2 knockout relative to wild-type controls (Figure 6A).

Gene set enrichment analysis (GSEA) identified multiple functional gene sets significantly enriched in ARG2-deficient CAR-T cells, including the PI3K-AKT signaling pathway, signaling pathways regulating stem cell pluripotency, and glycine-serine-threonine metabolism (Figure 6B–E).

Examination of individual differentially expressed genes confirmed elevated expression of key effector molecules in ARG2 knockout cells, including the cytokines TNF and IFNG, the cytolytic mediators PRF1 and GNLY, and additional functional regulators TNFSF14 and ABCG1 [17–20] (Figure 6F). Given the prominent enrichment of the PI3K-AKT signaling pathway, we selected IGF2 a key upstream activator of this axis for further validation. TPM-normalized RNA-seq data confirmed that IGF2 transcript levels were significantly elevated in ARG2-deficient CAR-T cells

(Figure 6G). Quantitative PCR independently verified this upregulation. Notably, pharmacological ARG2 inhibition with BEC in wild-type cells partially recapitulated the IGF2 induction observed in ARG2 knockout cells (Figure 6H), indicating that ARG2 enzymatic activity functionally restrains IGF2 expression.

Collectively, these findings suggest a potential regulatory cascade whereby ARG2 depletion may upregulate IGF2, a known activator of PI3K-AKT signaling, offering a molecular framework for understanding the enhanced effector function and metabolic fitness of ARG2-targeted CAR-T cells under hypoxia.

Discussion

Hypoxia is well recognized as a major metabolic barrier that impairs the persistence and anti-tumor potency of adoptively transferred CAR-T cells within solid tumor microenvironments. Previous immunometabolism studies have largely attributed arginine deprivation in tumor lesions to ARG1 overexpression by myeloid-derived suppressor cells and tumor stromal cells, which extrinsically restricts the proliferation and effector functions of tumor-infiltrating T lymphocytes [21–24]. However, most prior work focused on paracrine arginine depletion rather than cell-autonomous metabolic reprogramming mediated by intracellular ARG2 in T cells. A small body of research using conventional $CD8^+$ T cells has demonstrated that endogenous ARG2 independently regulates T cell activation, cytotoxicity and memory differentiation regardless of extracellular arginine availability, and genetic ablation of ARG2 remarkably improves the long-term anti-tumor durability of T cells and synergizes

521 with PD-1 blockade [25].

522 Extending these observations to genetically engineered CAR-T cells, the present
523 study confirmed that hypoxia markedly induced ARG2 transcription in two
524 independent CAR-T cell lines (MSLN-CAR and CD70-CAR) with identical
525 intracellular signaling domains, and such upregulation was independent of
526 CAR-targeted antigens. Prior studies have identified HIF-1α as a transcription factor
527 capable of driving ARG2 expression under low oxygen conditions [26]. Although we
528 did not further dissect the upstream transcription machinery governing ARG2 in
529 CAR-T cells, our observation of hypoxia-induced ARG2 upregulation aligns with the
530 general paradigm of hypoxia-mediated ARG2 induction.

531 The arginase inhibitor BEC has been widely used to probe the role of arginine
532 metabolism in immune regulation. Previous studies have shown that pharmacological
533 blockade of ARG2 by BEC restores intracellular arginine levels and reverses the
534 proliferative suppression of CD4+ T cells imposed by ARG2-expressing
535 myeloid-derived suppressor cells in inflammatory settings [16]. In tumor models,
536 BEC-mediated ARG2 inhibition has been reported to rescue CD8+ T cell glycolytic
537 capacity, proliferation and cytotoxic function that are impaired by tumor cell-derived
538 ARG2 [27,28]. However, most of these studies focused on paracrine arginine
539 depletion driven by myeloid or tumor cells, and whether direct inhibition of T
540 cell-intrinsic ARG2 by BEC can protect CAR-T cells from hypoxia-induced
541 dysfunction remains largely unexplored. In our study, ex vivo BEC pretreatment
542 significantly preserved serial killing capac integratingity and enhanced IFN-γ and

TNF-α secretion in hypoxic CAR-T cells, accompanied by reduced expression of the exhaustion markers PD-1 and LAG-3. These functional improvements are consistent with prior observations that arginase inhibition restores T cell effector function under arginine-deprived conditions [25,29,30]. More importantly, we found that BEC treatment further reshaped memory differentiation, increasing the proportion of stem cell memory and central memory subsets while decreasing terminal effector populations. This memory-promoting effect aligns with previous genetic studies showing that ARG2 deletion in conventional CD8+ T cells drives memory lineage commitment and enhances long-term antitumor persistence [25]. Our data extend these findings by demonstrating that pharmacological inhibition of ARG2 via BEC can recapitulate such memory-reprogramming effects in CAR-engineered T cells under hypoxic stress.

L-arginine, a conditionally essential amino acid that supports T cell activation and effector function, represents a widely investigated metabolic target for adoptive T cell therapy [31,32]. Exogenous L-arginine maintains amino acid bioavailability, supports mitochondrial oxidative phosphorylation, and enhances T cell cytotoxicity, pro-inflammatory cytokine production, and in vivo antitumor persistence [33–35]. A recent study adopted a complementary engineering strategy, introducing arginine residues into the scFv light-chain framework of CAR constructs to enhance antigen-binding avidity, prolong in vivo persistence, and improve therapeutic outcomes [36]. Collectively, these findings establish arginine modulation as a broadly effective strategy to augment CAR-T cell performance. Given our earlier finding that

hypoxia robustly upregulates ARG2 in CAR-T cells, and that elevated ARG2 activity drives intracellular arginine hydrolysis and depletes cellular arginine pools, we hypothesized that exogenous L-arginine supplementation might compensate for this substrate loss and mitigate hypoxia-induced CAR-T cell dysfunction. In support of this hypothesis, our data demonstrate that L-arginine supplementation restored serial cytotoxicity, enhanced IFN-γ and TNF-α production, and reduced expression of the exhaustion markers PD-1 and LAG-3 in hypoxic CAR-T cells. These results confirm that arginine availability constitutes a limiting factor for CAR-T effector function under nutrient-deprived conditions, extending the established role of arginine in supporting conventional T cell effector responses to CAR-engineered T cells under hypoxic stress.

Notably, L-arginine supplementation did not induce memory subset remodeling in hypoxic CAR-T cells, despite its well-documented pro-memory effects under normoxic conditions [31]. Several factors may account for this discrepancy. First, hypoxic stress is known to drive terminal effector differentiation, which may override the pro-memory effects of exogenous arginine [37,38]. Second, our expansion-phase pretreatment regimen differs from the continuous supplementation used in most prior studies, though this procedural difference alone cannot explain the absent memory remodeling. Most importantly, our data revealed that hypoxia robustly induced ARG2 overexpression in CAR-T cells. The resultant ARG2 hyperactivity hydrolyzes intracellular arginine and diverts flux away from memory-associated biosynthetic pathways, such that extracellular arginine supplementation alone cannot fully

overcome this cell-intrinsic metabolic shunt. This notion is corroborated by our finding that pharmacological ARG2 inhibition by BEC, but not L-arginine, effectively reshaped memory differentiation under hypoxia. Collectively, these data indicate that L-arginine supplementation primarily rescues acute effector function, whereas direct ARG2 blockade is required to reprogram T cell fate under prolonged hypoxic stress.

Building on the in vitro functional improvements conferred by BEC inhibition and L-arginine supplementation, we next assessed their in vivo antitumor efficacy in the 1806 xenograft tumor model. Consistent with our in vitro observations, both BEC-pretreated and L-arginine-pretreated CAR-T cells exerted stronger tumor growth suppression compared with control CAR-T cells. The enhanced tumor control was accompanied by higher circulating CAR-T cell frequencies, reduced proportions of exhausted T cells, and increased intratumoral $CD45^+$ lymphocyte infiltration. Notably, the memory-reprogramming effect of BEC was maintained in vivo, with elevated central memory and reduced terminal effector subsets among circulating CAR-T cells. This in vitro–in vivo concordance supports that BEC induces durable phenotypic remodeling rather than transient functional enhancement.

From a translational perspective, ex vivo pretreatment of CAR-T cells before infusion offers distinct advantages over systemic drug administration or continuous amino acid supplementation, including more precise dose control, lower risk of systemic metabolic disturbance, and better compatibility with current CAR-T manufacturing protocols. In accordance with good tolerability, no obvious body weight loss or histopathological damage in major organs was observed across all treatment groups.

These findings align with a growing body of preclinical studies demonstrating that metabolic interventions targeting amino acid metabolism enhance CAR-T cell persistence and tumor infiltration in solid tumor xenograft models [29,39], further validating metabolic optimization as a promising strategy to improve CAR-T therapy against solid tumors. It should be noted, however, that our immunodeficient xenograft model cannot fully reflect the interplay between ARG2-targeted CAR-T cells and the endogenous immune system, which warrants further validation in immunocompetent tumor models.

Genetic deletion of ARG2 has been proposed as a durable approach to enhance T cell-based immunotherapy. Previous work in unmodified $CD8^+$ T cells has shown that ARG2 knockout improves long-term antitumor persistence and synergizes with immune checkpoint blockade [25,27], but whether this strategy is equally effective in CAR-T cells, especially under hypoxic stress, had not been addressed. Using CRISPR-Cas9-mediated gene editing, we found that ARG2 ablation in CAR-T cells largely recapitulated the protective phenotypes observed with BEC treatment, including preserved cytolytic activity, reduced exhaustion and an increased CD62L-positive memory-like population under hypoxia. The high concordance between pharmacological inhibition and genetic knockout provides strong evidence that the observed benefits are specifically mediated by ARG2 targeting rather than off-target effects of small molecules. Our findings therefore confirm and extend the role of ARG2 as a cell-intrinsic negative regulator of T cell fitness to the context of CAR-T cells and hypoxic stress. Interestingly, one knockout clone with only partial

ARG2 protein reduction still exhibited significant functional improvements. This observation has practical relevance for clinical translation, as uniform biallelic knockout is often difficult to achieve in large-scale clinical manufacturing, and our data suggest that even partial ARG2 knockdown is sufficient to confer therapeutic benefits.

To explore the molecular underpinnings of ARG2-mediated CAR-T cell regulation, we performed transcriptomic profiling of ARG2 knockout CAR-T cells. GSEA revealed significant enrichment of the PI3K-AKT signaling pathway. While chronic PI3K-AKT activation is typically associated with CAR-T exhaustion and terminal effector differentiation, pharmacological inhibition of this axis during ex vivo expansion has been shown to preserve stem cell memory (TSCM) phenotypes and enhance persistence [40–43]. Our data suggest that ARG2 loss may induce a metabolically primed state of PI3K-AKT signaling that supports metabolic fitness without triggering terminal differentiation. We also observed enrichment of signaling pathways regulating stem cell pluripotency. The Wnt/β-catenin axis is a well-established determinant of T cell stemness; GSK3β inhibitors such as TWS119 have been employed in clinical-grade CAR-T manufacturing to enrich TSCM populations and improve therapeutic durability [44,45]. The upregulation of this pathway in ARG2-deficient cells indicates that ARG2 deletion transcriptionally reprograms CAR-T cells toward a less differentiated, stem-like state. Beyond signaling, ARG2 deletion triggered metabolic reprogramming, as evidenced by enrichment of glycine, serine, and threonine metabolism. This pathway fuels

one-carbon metabolism and redox homeostasis; its upregulation suggests enhanced metabolic plasticity to withstand nutrient deprivation and hypoxic stress within solid tumors [46–48]. Differential expression analysis further identified coordinated upregulation of key effector genes including TNF, TNFSF14 (LIGHT), IFNG, ABCG1, PRF1, and GNLY, demonstrating that ARG2 deficiency reinforces cytotoxic potential while simultaneously promoting memory-associated programs. Finally, targeted validation confirmed marked upregulation of IGF2, a key upstream activator of the PI3K-AKT axis [49,50]. Emerging evidence indicates that IGF2 regulates T cell proliferation and glucose metabolism [51,52], and its robust induction in ARG2-KO cells suggests it may function as a metabolic checkpoint linking arginine metabolism to T cell growth and memory persistence. In summary, ARG2 deletion orchestrates multi-layered reprogramming encompassing PI3K-AKT signaling, stem cell-associated pathways, glycine/serine/threonine metabolism, and effector molecule expression. These findings nominate druggable pathways—such as Wnt activation and IGF2 signaling—that could be strategically combined with ARG2 modulation to optimize CAR-T metabolic fitness and therapeutic durability.

While our findings establish ARG2 as a cell intrinsic metabolic checkpoint governing hypoxic CAR-T cell function, several key points remain to be further explored. Our in-vivo studies rely on immunodeficient xenograft models, which cannot fully recapitulate crosstalk with endogenous host immunity. Additionally, transcriptomic analyses imply that IGF2 upregulation may mediate PI3K-AKT pathway activation upon ARG2 loss; however, this correlative observation requires formal functional

validation. Despite these considerations, our work provides a compelling preclinical rationale for ex-vivo ARG2 modulation to enhance CAR-T fitness in hypoxic solid tumors, with further preclinical work needed before clinical translation.

Conclusions

In conclusion, our study establishes ARG2 as a critical mediator of hypoxia-driven CAR-T cell dysfunction and identifies ARG2-targeted interventions as a practical strategy to enhance CAR-T cell resistance to hypoxic stress. Pharmacological inhibition with BEC, L-arginine supplementation, and genetic ARG2 knockout each effectively improve effector function under low-oxygen conditions, with BEC treatment uniquely conferring a favorable memory phenotype. Our results also demonstrate that ARG2 modulation effectively alleviates hypoxia-induced exhaustion and preserves antitumor activity in preclinical mouse models. Together, these findings provide a compelling rationale for integrating pharmacological ARG2 preconditioning or genetic ARG2 ablation into CAR-T cell culturing to improve their performance in hypoxia tumor micro environment.

References

[1] K. Ai, B. Liu, X. Chen, C. Huang, liping Yang, W. Zhang, J. Weng, X. Du, K. Wu, and P. Lai, Optimizing CAR-T cell therapy for solid tumors: current challenges and potential strategies, J. Hematol. Oncol.J Hematol Oncol **17**, 105 (2024).

[2] B. Wang, Q. Zhao, Y. Zhang, Z. Liu, Z. Zheng, S. Liu, L. Meng, Y. Xin, and X. Jiang, Targeting hypoxia in the tumor microenvironment: a potential strategy to improve cancer immunotherapy, J. Exp. Clin. Cancer Res. **40**, 24 (2021).

[3] G. L. Semenza, Intratumoral Hypoxia and Mechanisms of Immune Evasion Mediated by Hypoxia-Inducible Factors, Physiology **36**, 73 (2021).

[4] R. Berahovich, X. Liu, H. Zhou, E. Tsadik, S. Xu, V. Golubovskaya, and L. Wu, Hypoxia Selectively Impairs CAR-T Cells In Vitro, Cancers **11**, 602 (2019).

[5] C. del M. A. Pauneto et al., Intra-tumoral hypoxia promotes CD8+ T cell dysfunction via chronic activation of integrated stress response transcription factor ATF4, Immunity **58**, 2489

(2025).
[6] M. Zhou, L. Xu, J. Hu, W. Chen, J. Hong, M. Wang, and Z. Guo, Metabolic reprogramming through PIM3 inhibition reverses hypoxia-induced CAR-T cell dysfunction in solid tumors, J. Transl. Med. **23**, 1230 (2025).
[7] H. Wu et al., Mitochondrial dysfunction promotes the transition of precursor to terminally exhausted T cells through HIF-1α-mediated glycolytic reprogramming, Nat. Commun. **14**, 6858 (2023).
[8] X. Zhu et al., Hypoxia-Responsive CAR-T Cells Exhibit Reduced Exhaustion and Enhanced Efficacy in Solid Tumors, Cancer Res. **84**, 84 (2024).
[9] W. Li et al., Envirotune-CAR-T: a hypoxia-responsive and glutamine-enhanced CAR-T cell therapy for overcoming tumor microenvironment-mediated suppression, J. Immunother. Cancer **13**, e012321 (2025).
[10] H. rong Li, J. Xiong, C. hui Wang, L. bing Hu, Y. bao Wang, Q. rong Ping, M. Yang, J. Tan, T. ting Li, and Y. Yang, CAR-T cell therapy for solid tumors: HIF-1α as a potential enhancement strategy, Autoimmunity **58**, 2579069 (2025).
[11] W. Deng, C. Li, Q. Wang, X. Jiang, and Y. Xie, CD8+ T cell exhaustion driven by metabolic reprogramming, Cancer Cell Int. **26**, 194 (2026).
[12] B. Akbari, Z. Hosseini, P. Shahabinejad, S. Ghassemi, H. R. Mirzaei, and R. S. O'Connor, Metabolic and epigenetic orchestration of (CAR) T cell fate and function, Cancer Lett. **550**, 215948 (2022).
[13] S. Liu et al., β-hydroxybutyrate enhances the metabolic fitness of CAR T cells in cancer, Cell **189**, 1701 (2026).
[14] D. Pandey et al., Hypoxia Triggers SENP1 (Sentrin-Specific Protease 1) Modulation of KLF15 (Kruppel-Like Factor 15) and Transcriptional Regulation of Arg2 (Arginase 2) in Pulmonary Endothelium, Arterioscler. Thromb. Vasc. Biol. **38**, 913 (2018).
[15] B. Chen, Y. Jin, C. M. Pool, Y. Liu, and L. D. Nelin, Hypoxic pulmonary endothelial cells release epidermal growth factor leading to vascular smooth muscle cell arginase-2 expression and proliferation, Physiol. Rep. **10**, e15342 (2022).
[16] Q. Long et al., Pharmacological and genetic inhibition of ARG2 in $CXCR2^{Hi}$ myeloid-derived suppressor cells combats sepsis-induced lymphopenia, Theranostics **15**, 7990 (2025).
[17] S. Ghosh et al., T-cell gene therapy for perforin deficiency corrects cytotoxicity defects and prevents hemophagocytic lymphohistiocytosis manifestations, J. Allergy Clin. Immunol. **142**, 904 (2018).
[18] M. Walch, F. Dotiwala, S. Mulik, J. Thiery, T. Kirchhausen, C. Clayberger, A. M. Krensky, D. Martinvalet, and J. Lieberman, Cytotoxic Cells Kill Intracellular Bacteria through Granulysin-Mediated Delivery of Granzymes, Cell **157**, 1309 (2014).
[19] C. F. Ware, M. Croft, and G. A. Neil, Realigning the LIGHT signaling network to control dysregulated inflammation, J. Exp. Med. **219**, e20220236 (2022).
[20] H.-Y. Cheng, D. E. Gaddis, R. Wu, C. McSkimming, L. D. Haynes, A. M. Taylor, C. A. McNamara, M. Sorci-Thomas, and C. C. Hedrick, Loss of ABCG1 influences regulatory T cell differentiation and atherosclerosis, J. Clin. Invest. **126**, 3236 (n.d.).
[21] Z. Liu, Single-Cell RNA Sequencing Reveals Immunosuppressive Mechanisms of MDSCs in Lung Cancer, BIO Web Conf. **174**, 01016 (2025).
[22] E. Jou, N. Chaudhury, and F. Nasim, Novel therapeutic strategies targeting myeloid-derived

suppressor cell immunosuppressive mechanisms for cancer treatment, Explor. Target. Anti-Tumor Ther. **5**, 187 (2024).
[23] Z. Zhao et al., FFAR2 expressing myeloid-derived suppressor cells drive cancer immunoevasion, J. Hematol. Oncol.J Hematol Oncol **17**, 9 (2024).
[24] M. S. Kim, H. Kang, J.-H. Baek, M.-G. Cho, E. J. Chung, S.-J. Kim, J.-Y. Chung, and K.-H. Chun, Disrupting Notch signaling related HES1 in myeloid cells reinvigorates antitumor T cell responses, Exp. Hematol. Oncol. **13**, 122 (2024).
[25] A.-A. Martí I Líndez et al., Mitochondrial arginase-2 is a cell-autonomous regulator of CD8+ T cell function and antitumor efficacy, JCI Insight **4**, e132975 (2019).
[26] X. Liang, D. M. Potenza, A. Brenna, Y. Ma, Z. Ren, X. Cheng, X.-F. Ming, and Z. Yang, Hypoxia Induces Renal Epithelial Injury and Activates Fibrotic Signaling Through Up-Regulation of Arginase-II, Front. Physiol. **12**, (2021).
[27] L. Cai, Y. Cao, J. Zhang, K. Xi, A. Li, and H. Zhang, Inhibiting Arginine Metabolism via ALDH2/ARG2 Axis Blockade Potentiates Immune Checkpoint Inhibitors in Colorectal Cancer, Mol. Cancer Ther. **24**, 1977 (2025).
[28] B. Érsek, P. Silló, U. Cakir, V. Molnár, A. Bencsik, B. Mayer, E. Mezey, S. Kárpáti, Z. Pós, and K. Németh, Melanoma-associated fibroblasts impair CD8+ T cell function and modify expression of immune checkpoint regulators via increased arginase activity, Cell. Mol. Life Sci. **78**, 661 (2021).
[29] S. M. Steggerda et al., Inhibition of arginase by CB-1158 blocks myeloid cell-mediated immune suppression in the tumor microenvironment, J. Immunother. Cancer **5**, (2017).
[30] X. Zhu, J. P. Pribis, P. C. Rodriguez, S. M. Morris, Y. Vodovotz, T. R. Billiar, and J. B. Ochoa, The Central Role of Arginine Catabolism in T-Cell Dysfunction and Increased Susceptibility to Infection After Physical Injury, Ann. Surg. **259**, 171 (2014).
[31] R. Geiger et al., L-Arginine Modulates T Cell Metabolism and Enhances Survival and Anti-tumor Activity, Cell **167**, 829 (2016).
[32] Y. Zhou et al., Metabolic conditioning for enhanced CAR T cell function, Blood **146**, 4127 (2025).
[33] R. J. Kishton, M. Sukumar, and N. P. Restifo, Arginine Arms T Cells to Thrive and Survive, Cell Metab. **24**, 647 (2016).
[34] L. Yang, Z. Chu, M. Liu, Q. Zou, J. Li, Q. Liu, Y. Wang, T. Wang, J. Xiang, and B. Wang, Amino acid metabolism in immune cells: essential regulators of the effector functions, and promising opportunities to enhance cancer immunotherapy, J. Hematol. Oncol.J Hematol Oncol **16**, 59 (2023).
[35] W. Li et al., Cell metabolism-based optimization strategy of CAR-T cell function in cancer therapy, Front. Immunol. **14**, (2023).
[36] S. Maeta, A. Fukunaga, Y. Egashira, Y. Akahori, L. Wang, N. Seo, Y. Atarashi, D. Ejima, H. Fujiwara, and H. Shiku, Introducing arginine residues into scFv in CAR-T cells shows promising antitumor effects, Mol. Ther. **34**, 1421 (2026).
[37] M. Davern et al., Nutrient deprivation and hypoxia alter T cell immune checkpoint expression: potential impact for immunotherapy, J. Cancer Res. Clin. Oncol. **149**, 5377 (2023).
[38] A. T. Phan, A. L. Doedens, A. Palazon, P. A. Tyrakis, K. P. Cheung, R. S. Johnson, and A. W. Goldrath, Constitutive Glycolytic Metabolism Supports CD8+ T Cell Effector Memory Differentiation during Viral Infection, Immunity **45**, 1024 (2016).
[39] L. Fultang et al., Metabolic engineering against the arginine microenvironment enhances

CAR-T cell proliferation and therapeutic activity, Blood **136**, 1155 (2020).
[40] W. Zhang, X. Zhang, L. Hu, S. Jin, L. Pitts, M. Kofler, Z. Wang, J. Iske, Y. Nian, and Z. Shen, Idelalisib modulates CD4+ T cell responses to mitigate rejection of allografts in mice, Int. Immunopharmacol. **162**, 115155 (2025).
[41] W. Zheng, C. E. O'Hear, R. Alli, J. H. Basham, H. A. Abdelsamed, L. E. Palmer, L. L. Jones, B. Youngblood, and T. L. Geiger, PI3K orchestration of the in vivo persistence of chimeric antigen receptor-modified T cells, Leukemia **32**, 1157 (2018).
[42] C. R. Funk et al., PI3Kδ/γ inhibition promotes human CART cell epigenetic and metabolic reprogramming to enhance antitumor cytotoxicity, Blood **139**, 523 (2022).
[43] R. Urak, M. Walter, L. Lim, C. W. Wong, L. E. Budde, S. Thomas, S. J. Forman, and X. Wang, Ex vivo Akt inhibition promotes the generation of potent CD19CAR T cells for adoptive immunotherapy, J. Immunother. Cancer **5**, (2017).
[44] L. Gattinoni et al., Wnt signaling arrests effector T cell differentiation and generates CD8+ memory stem cells, Nat. Med. **15**, 808 (2009).
[45] M. Sabatino et al., Generation of clinical-grade CD19-specific CAR-modified CD8+ memory stem cells for the treatment of human B-cell malignancies, Blood **128**, 519 (2016).
[46] E. H. Ma et al., Serine Is an Essential Metabolite for Effector T Cell Expansion, Cell Metab. **25**, 345 (2017).
[47] N. Ron-Harel et al., Mitochondrial Biogenesis and Proteome Remodeling Promote One-Carbon Metabolism for T Cell Activation, Cell Metab. **24**, 104 (2016).
[48] D. Aviles-Huerta et al., Dual Ribosome Profiling reveals metabolic limitations of cancer and stromal cells in the tumor microenvironment, Nat. Commun. **16**, 4652 (2025).
[49] Q. Mu et al., Imp2 regulates GBM progression by activating IGF2/PI3K/Akt pathway, Cancer Biol. Ther. **16**, 623 (2015).
[50] H. Yang et al., Brushite-coated Mg–Nd–Zn–Zr alloy promotes the osteogenesis of vertebral laminae through IGF2/PI3K/AKT signaling pathway, Biomater. Adv. **152**, 213505 (2023).
[51] D. Song et al., Insulin-like growth factor 2 drives fibroblast-mediated tumor immunoevasion and confers resistance to immunotherapy, J. Clin. Invest. **134**, (2024).
[52] W.-K. Hofmann, S. Takeuchi, M. A. Frantzen, D. Hoelzer, and H. P. Koeffler, Loss of genomic imprinting of insulin-like growth factor 2 is strongly associated with cellular proliferation in normal hematopoietic cells, Exp. Hematol. **30**, 318 (2002).

Figures

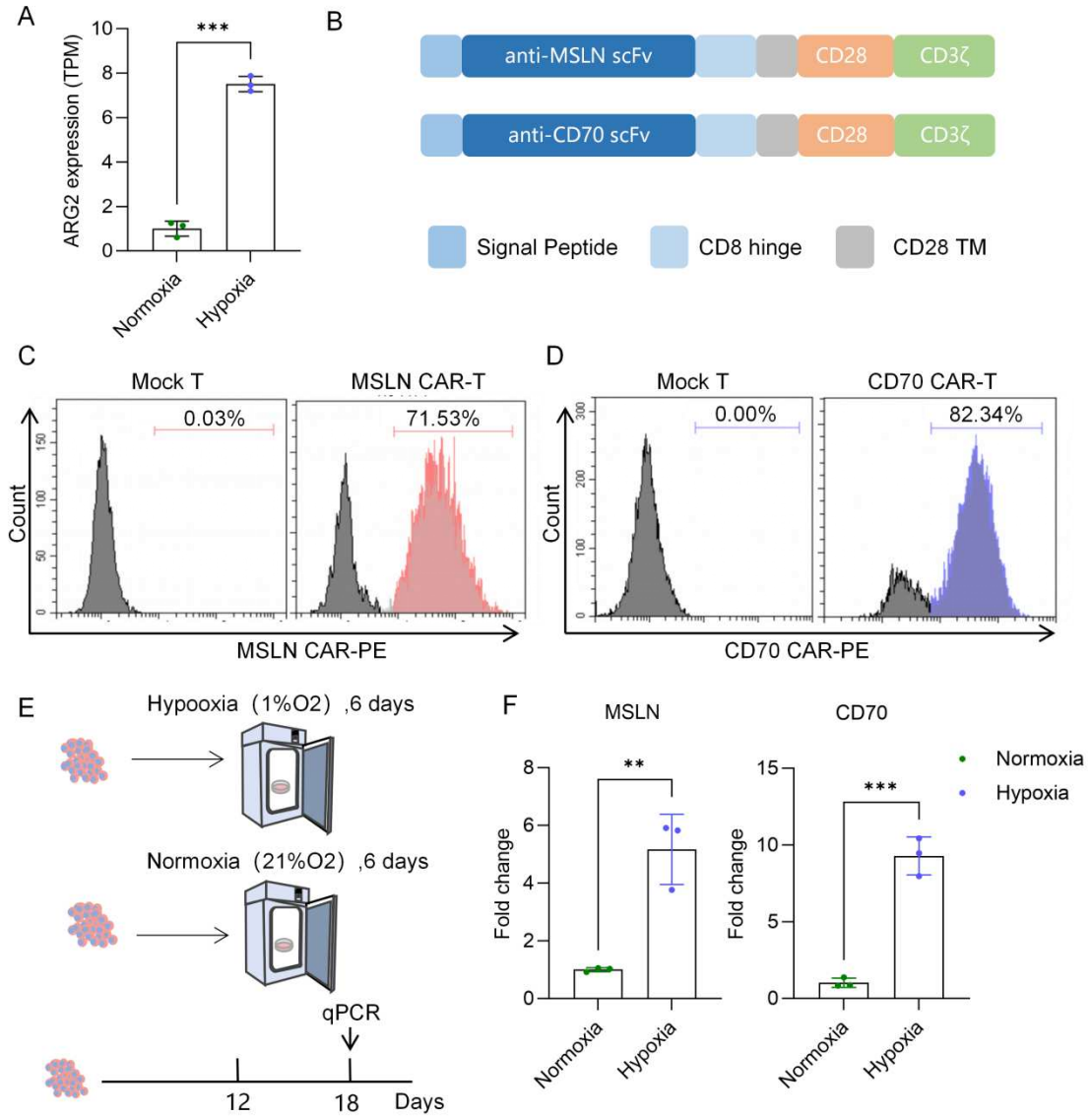


Figure 1. Construction and validation of MSLN and CD70 CAR-T cells and hypoxia-induced ARG2 upregulation. (A) ARG2 transcript levels in T cells under normoxic and hypoxic conditions detected by transcriptome sequencing. (B) Schematic representation of MSLN-CAR and CD70-CAR constructs, both containing a CD8α signal peptide, antigen-specific scFv, CD8α hinge, CD28 transmembrane domain, CD28 costimulatory domain, and CD3ζ signaling domain. (C) Flow cytometric analysis of CAR surface expression in Mock T cells and MSLN CAR-T cells. (D) Flow cytometric analysis of CAR surface expression in Mock T

cells and CD70 CAR-T cells. (E) Experimental scheme showing CAR-T cell culture and subsequent hypoxic exposure. (F) qPCR analysis of ARG2 mRNA levels in MSLN-CAR-T and CD70-CAR-T cells under normoxic and hypoxic conditions. Data represent mean ± SD from three independent experiments. Statistical significance was determined using a two-tailed unpaired t-test. $^{**}P < 0.01$; $^{***}P < 0.001$.

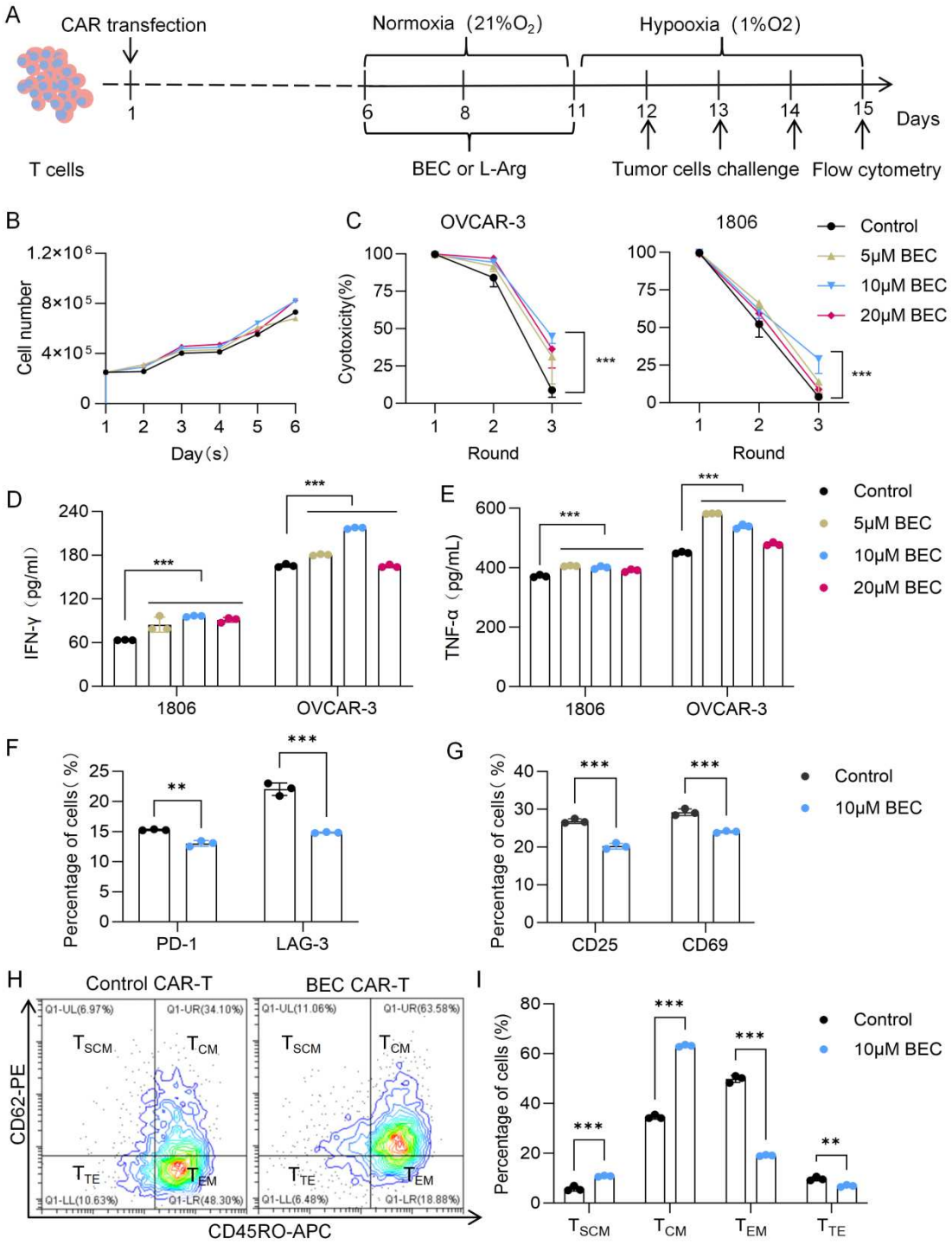
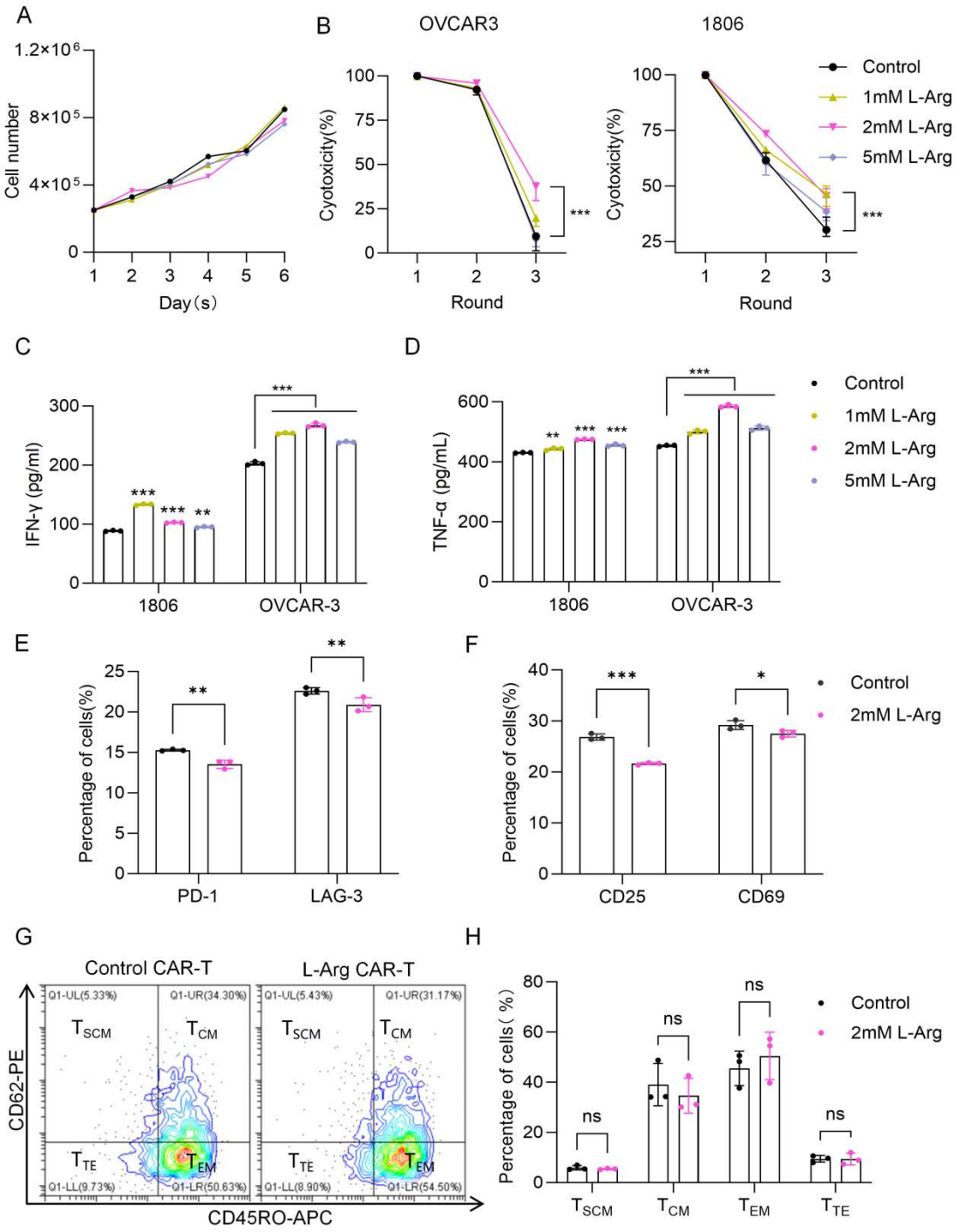


Figure 2. Pharmacological inhibition of ARG2 by BEC restores antitumor effector function and modulates phenotypic profiles of CAR-T cells under hypoxic conditions in vitro. (A) Schematic representation of the experimental timeline. CAR-T cells were treated with BEC or L-arginine (L-Arg) from day 6 to day 11 post-transfection,

842 after which the medium was refreshed to remove residual compounds, and cells were transferred
843 to hypoxic conditions (1% O_2) for subsequent functional assessments. (B) Proliferation of CAR-T
844 cells treated with different concentrations of BEC (5, 10, 20 μM) was monitored over 6 days. (C)
845 Cytotoxic activity of hypoxic CAR-T cells against OVCAR3 and 1806 ovarian cancer cell lines
846 was measured in a multi-round serial killing assay. (D-E) Secretion levels of the pro-inflammatory
847 cytokines IFN-γ (D) and TNF-α. (E) by hypoxic CAR-T cells were detected after co-culture with
848 1806 or OVCAR3 tumor cells. (F) Surface expression of T cell exhaustion markers PD-1 and
849 LAG-3 on hypoxic CAR-T cells with or without 10 μM BEC treatment. (G) Surface expression of
850 T cell activation markers CD25 and CD69 on hypoxic CAR-T cells with or without 10 μM BEC
851 treatment. (H) Memory phenotype of hypoxic CAR-T cells was analyzed based on CD62L and
852 CD45RO expression. Left: Representative flow cytometry plots; Right: Statistical analysis of stem
853 cell memory (T_{SCM}), central memory (T_{CM}), effector memory (T_{EM}) and terminal effector (T_{TE})
854 subsets. Data represent mean ± SD from three independent experiments. Statistical significance
855 was determined using two-way ANOVA (B, C), one-way ANOVA (D, E), and two-tailed unpaired
856 t-test (F, G, H). $^{**}P < 0.01$; $^{***}P < 0.001$.
857



858

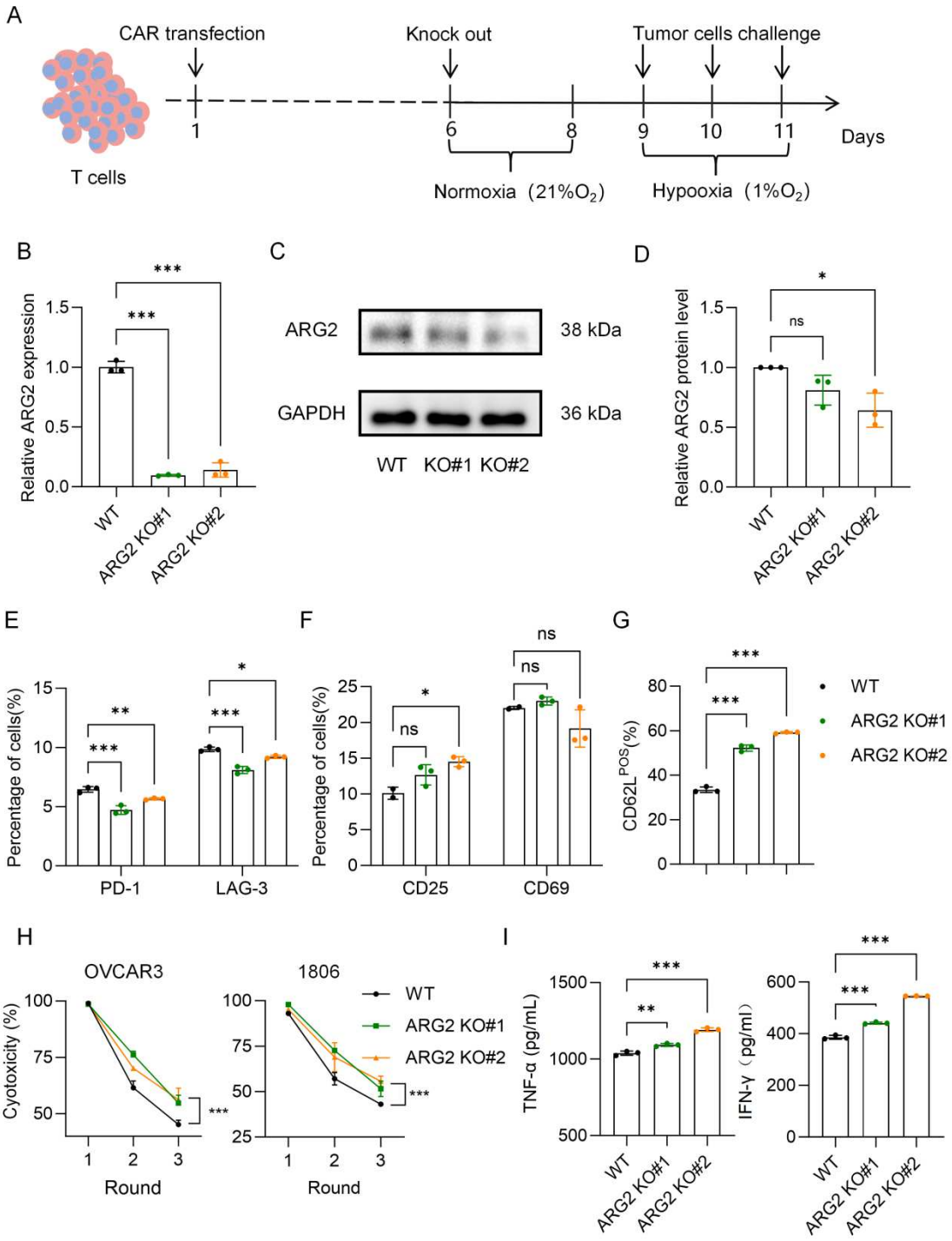
859 **Figure 3. L-Arginine supplementation restores the cytotoxic function, cytokine**

860 **secretion and exhaustion phenotypes of hypoxic CAR-T cells.** (A) Proliferation of

861 CAR-T cells treated with different concentrations of L-arginine (1, 2, 5 mM) was monitored over

862 6 days. (B) Cytotoxic activity of CAR-T cells against OVCAR3 and 1806 tumor cell lines was

863 measured in a multi-round serial killing assay. (C-D) Secretion levels of the pro-inflammatory
864 cytokines IFN-γ (C) and TNF-α (D) by CAR-T cells were detected after co-culture with 1806 or
865 OVCAR3 tumor cells. (E) Surface expression of T cell exhaustion markers PD-1 and LAG-3 on
866 CAR-T cells with or without 2 mM L-arginine treatment. (F) Surface expression of T cell
867 activation markers CD25 and CD69 on CAR-T cells with or without 2 mM L-arginine treatment.
868 (G-H) Memory phenotype of CAR-T cells was analyzed based on CD62L and CD45RO
869 expression. Left: Representative flow cytometry plots; Right: Statistical analysis of stem cell
870 memory (TSCM), central memory (TCM), effector memory (TEM) and terminal effector (TE)
871 subsets. Data represent mean ± SD from three independent experiments. Statistical significance
872 was determined using two-way ANOVA (A, B), one-way ANOVA (C, D), and two-tailed unpaired
873 t-test (E, F, H). *$P < 0.05$; **$P < 0.01$; ***$P < 0.001$; ns, not significant.



874

875 **Fig. 4. Genetic ablation of ARG2 enhances the cytotoxic function, cytokine**

876 **secretion and memory phenotype of hypoxic CAR-T cells.** (A) Schematic diagram of

877 the experimental timeline and treatment protocol. Primary T cells were transfected with CAR on

878 day 1, followed by ARG2 knockout on day 6. Cells were cultured under normoxia (21% O_2) from

day 6 to day 8, and then subjected to repeated tumor cell challenge under hypoxic conditions (1% O_2). (B) Relative mRNA expression of ARG2 in wild-type (WT) and two independent ARG2 knockout (ARG2 KO#1, ARG2 KO#2) CAR-T cells, determined by quantitative PCR. (C) Representative Western blot image showing ARG2 protein levels in WT and ARG2 knockout CAR-T cells. (D) Densitometric quantification of ARG2 protein normalized to GAPDH from Western blot analysis. (E) Surface expression of T cell exhaustion markers PD-1 and LAG-3 on WT and ARG2 knockout CAR-T cells under hypoxic conditions. (F) Surface expression of T cell activation markers CD25 and CD69 on WT and ARG2 knockout CAR-T cells under hypoxic conditions. (G) Percentage of CD62L-positive cells in WT and ARG2 knockout CAR-T cells under hypoxic conditions, reflecting memory phenotype regulation. (H) Cytotoxic activity of WT and ARG2 knockout CAR-T cells against OVCAR3 and 1806 tumor cell lines, measured in a multi-round serial killing assay under hypoxia. (I) Secretion levels of the pro-inflammatory cytokines TNF-α and IFN-γ by CAR-T cells were detected after co-culture with tumor cells under hypoxic conditions. Data represent mean ± SD from three independent experiments. Statistical significance was determined using two-way ANOVA (H), and one-way ANOVA (B, E, F, G, I). *$P < 0.05$; **$P < 0.01$; ***$P < 0.001$; ns, not significant.

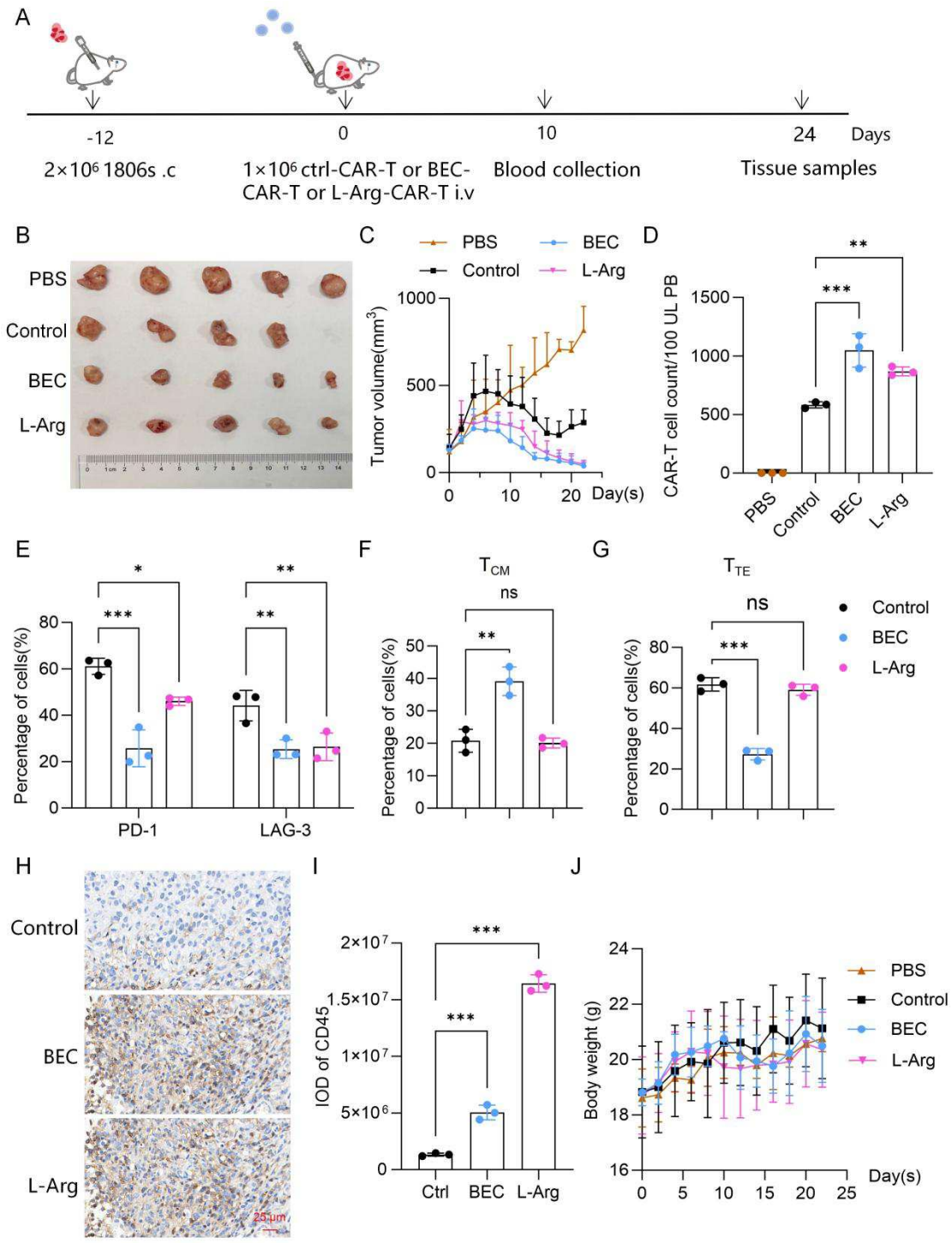
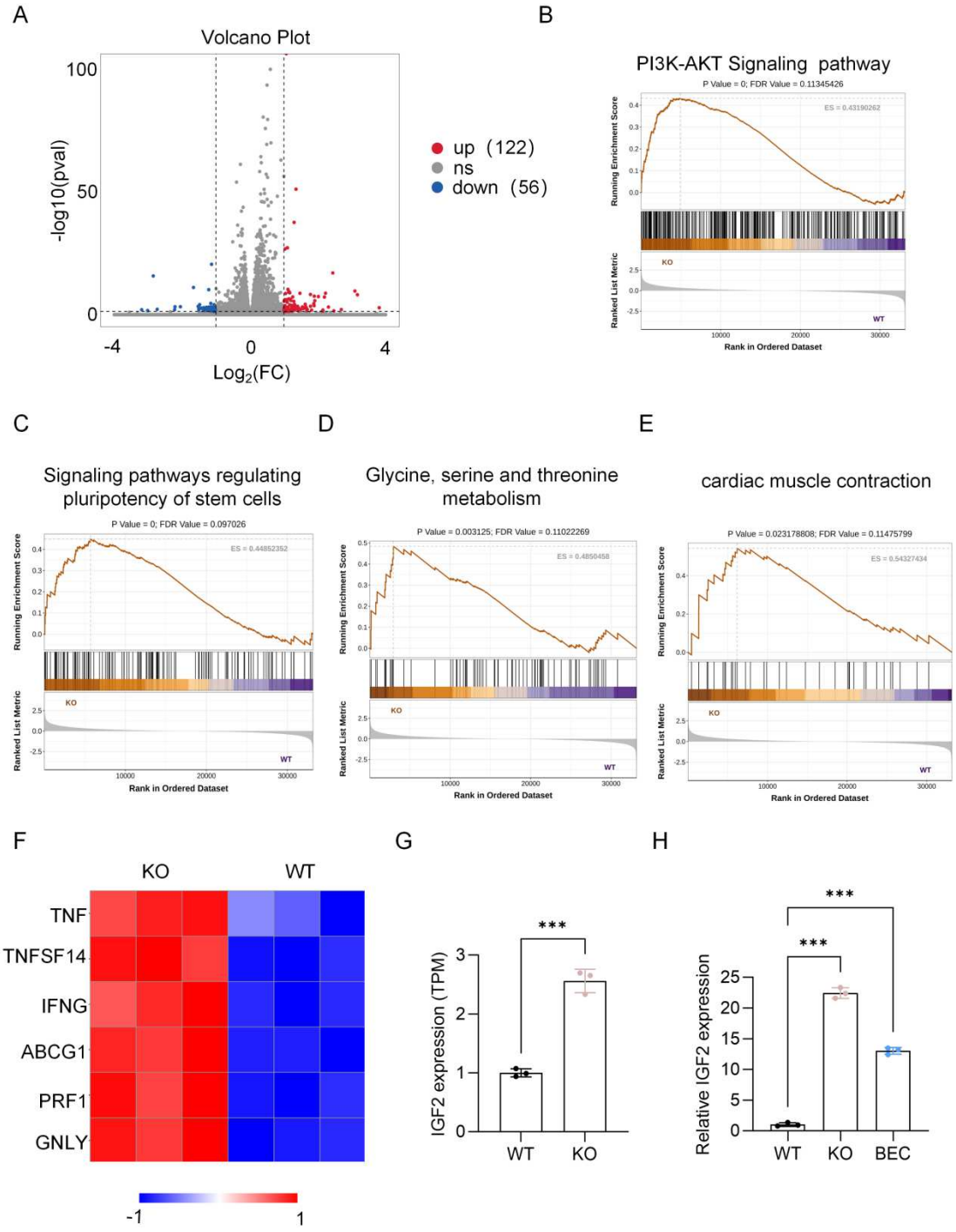


Fig. 5. In vivo efficacy, circulating CAR-T abundance, and T-cell phenotypic remodeling of ARG2-modulated CAR-T cells in the 1806 xenograft model. (A) Schematic overview of the xenograft tumor model and in vivo experimental timeline. 1806 tumor bearing mice received intravenous injection of control CAR -T, BEC pretreated CAR-T or L-Arg

pretreated CAR-T cells. Peripheral blood and tumor tissues were collected at indicated time-points. (B) Representative images of xenograft tumors harvested from each group (n = 5). (C) Tumor volume growth curves of tumor bearing mice in different groups. (D) Quantification of circulating CAR-T cell counts in mouse peripheral blood at day 10 post adoptive transfer. (E) Percentages of PD-1 and LAG-3 positive CAR-T cells isolated from peripheral blood. (F-G) Frequency of T_{CM} and T_{TE} subsets within circulating CAR-T cells. (H) Representative immunohistochemical staining images of human CD45 in tumor sections, scale bar = 200 μm. (I) Quantitative analysis of integrated optical density (IOD) for intratumoral CD45 staining. (J) Body weight changes of mice during the experiment. Data are presented as mean ± SD. Statistical analyses were performed using one-way ANOVA (D-G, I) and two-way ANOVA (C, J). *$P < 0.05$; **$P < 0.01$; ***$P < 0.001$; ns, not significant.



911

912

913 **Figure 6. Transcriptomic profiling identifies transcriptional reprogramming**

914 **triggered by ARG2 deletion in hypoxic CAR-T cells.** (A) Volcano plot displaying

915 differentially expressed genes (DEGs) between wild-type (WT) and ARG2-knockout (KO)

CAR-T cells under hypoxia. Red dots denote significantly upregulated genes (n=122), blue dots represent significantly downregulated genes (n=56), and gray dots indicate non-significant genes (ns). (B-E) Gene set enrichment analysis (GSEA) plots showing enriched pathways in ARG2-KO CAR-T cells, including the PI3K-AKT signaling pathway (B), signaling pathways regulating pluripotency of stem cells (C), glycine, serine and threonine metabolism (D), and cardiac muscle contraction (E). Running enrichment scores and FDR values are presented for each signature. (F) Heatmap illustrating the relative expression of representative effector and immunomodulatory genes (TNF, TNFSF14, IFNG, ABCG1, PRF1, GNLY) in WT and ARG2-KO groups. Color scale ranges from-1 (blue) to 1 (red). (G) Transcriptomic (TPM) quantification of IGF2 expression in WT versus ARG2-KO CAR-T cells. (H) Relative IGF2 mRNA levels measured by qPCR in WT, ARG2-KO, and BEC-pretreated CAR-T cells. Data represent mean ± SD. Statistical analysis was performed with an appropriate test. ***$P < 0.001$.

Supplementary Files

This is a list of supplementary files associated with this preprint. Click to download.

- aarg2m1.png
- agapdhm.tif
- arg22m1.png
- barg22m1.png
- bgapdhm.tif
- gapdhm.tif
- supplementarymaterials.docx